Bioelectromagnetics 27:628–640 (2006)

Effects of a Moderate-Intensity Static Magnetic Field on VEGF-A Stimulated Endothelial Capillary Tubule Formation In Vitro

Hideyuki Okano,[1,2]* Rie Onmori,[1,2] Naohide Tomita,[1] and Yoshito Ikada[3]

[1]*International Innovation Center, Kyoto University, Kyoto, Japan*
[2]*Department of Science, Pip Tokyo Co., Ltd., Tokyo, Japan*
[3]*Faculty of Medical Engineering, Suzuka University of Medical Science, Mie, Japan*

Effects of a moderate-intensity static magnetic field (SMF) on the early-stage development of endothelial capillary tubule formation were examined during the initial cell growth periods using co-cultured human umbilical vein endothelial cells and human diploid fibroblasts. The co-cultured cells within a well (16 mm in diameter) were exposed to SMF intensity up to 120 mT (B_{max}) with the maximum spatial gradient of 21 mT/mm using a disc-shaped permanent magnet (16 mm in diameter and 2.5 mm in height) for up to 10 days. Control exposure was performed without magnet. Some vascular endothelial cells were treated with vascular endothelial growth factor (VEGF)-A (10 ng/ml) to promote the tubule formation every 2–3 days. Four experimental protocols were performed: (1) non-exposure (control); (2) SMF exposure alone; (3) non-exposure with VEGF-A; (4) SMF exposure with VEGF-A. Photomicrographs of tubule cells immunostained with an anti-platelet-endothelial cell adhesion molecule-1 (PECAM-1 [CD31]) antibody as a pan-endothelial marker, were analyzed after culture at 37 °C for 4, 7, and 10 days. The mean values of the area density and the length of tubules (related mainly to arteriogenesis) as well as the number of bifurcations (related mainly to angiogenesis) were determined as parameters of tubule formation and were compared between the groups. After a 10 day incubation, in the peripheral part of the culture wells, SMF alone significantly promoted the tubule formation in terms of the area density and the length of tubules, compared with control group. In the central part of the wells, however, SMF did not cause any significant changes in the parameters of tubule formation. After a 7 day incubation, VEGF-A significantly promoted all the parameters of tubule formation in any part of the wells, compared with control group. With regard to the synergistic effects of SMF and VEGF-A on tubule formation, after a 10 day incubation, SMF significantly promoted the VEGF-A-increased area density and length of tubules in the peripheral part of the wells, compared with the VEGF-A treatment alone. However, SMF did not induce any significant changes in the VEGF-A-increased number of bifurcations in any part of the wells. The tubule cells observed in the wells had elongated, spindle-like shapes, and the direction of cell elongation was random, irrespective of the presence and direction of SMF. These findings suggest that the application of SMF to intact or VEGF-A-stimulated vascular endothelial cells leads mainly to promote or enhance arteriogenesis in the peripheral part of the wells, where the spatial gradient increases relative to the central part. The effects of SMF on the VEGF-A-enhanced tubule formation appear to be synergistic or additive in arteriogenesis but not in angiogenesis. Bioelectromagnetics 27:628–640, 2006.

Key words: DC magnetic fields; tubule formation; VEGF-A; in vitro; magnetic field gradient

INTRODUCTION

Moderate-intensity static magnetic fields (SMF) ranging from 1 mT to 1 T have been shown to influence a wide variety of biological systems. Particularly, in the past decade, significant circulatory system responses to the moderate-intensity SMF have been reported in experimental animals in vivo [Saunders, 2005]: SMF

Grant sponsor: The Japan Society for the Promotion of Science; Grant numbers: JSPS-RFTF 96100203, JSPS-RFTF 98100201; Grant sponsor: Grant-in-Aid for Scientific Research (B).

*Correspondence to: Dr. Hideyuki Okano, Tomita Lab., Graduate School of Engineering (International Innovation Center [KU-IIC]), Kyoto University, Physics Building, Yoshida-Honmachi, Sakyo-ku, Kyoto 606-8317, Japan. E-mail: okano@iic.kyoto-u.ac.jp

Received for review 3 July 2005; Final revision received 20 March 2006

DOI 10.1002/bem.20246
Published online 12 July 2006 in Wiley InterScience (www.interscience.wiley.com).

exposure between 1 and 350 mT for anywhere between 10 min and 12 weeks influences cutaneous microcirculation and/or arterial blood pressure (BP) [Ohkubo and Xu, 1997; Xu et al., 1998, 2000; Okano et al., 1999, 2005a,b; Okano and Ohkubo, 2001, 2003a,b, 2005a,b; Gmitrov et al., 2002; Morris and Skalak, 2005], baroreflex sensitivity (BRS) [Gmitrov and Ohkubo, 2002a,b; Okano and Ohkubo, 2005a,b], heart rate [Veliks et al., 2004] and angiogenic response [Ruggiero et al., 2004].

Angiogenesis, the sprouting of new blood vessels, has become an important area of scientific research due to its involvement in various physiological and pathological processes [Ingber et al., 1990; Folkman, 1990, 1992; Folkman and Ingber, 1992; Leunig et al., 1992; Reynolds et al., 1992, 2002; Battegay, 1995; Arbiser, 1996; Boucher et al., 1996; Jain et al., 1996; Melder et al., 1996; Winet, 1996; Fukumura et al., 1998, 2001; Reynolds and Redmer, 1998; Carmeliet and Jain, 2000; Szekanecz and Koch, 2001; Jain, 2002, 2005; Szekanecz et al., 2005]. Angiogenesis is also critical for successful bone fracture healing [Donski et al., 1979; Steinbrech et al., 2000], but the effects of different kinds of magnetic fields on angiogenesis through vascular growth factors are inconsistent and contradictory. Prior to the studies of SMF, the effects of pulsed electromagnetic fields (PEMF) or electromagnetic fields (EMF) on angiogenesis have been studied in vitro and/or in vivo [Roland et al., 2000; Williams et al., 2001; Tepper et al., 2004]. One of the studies suggested that the application of PEMF (10–200 μT, 27.12 MHz, for 4–12 weeks) to a microsurgically-created arterial loop model increased the amount of neovascularization in vivo [Roland et al., 2000]. Another study suggested that PEMF (1.2 mT, 15 Hz, for 24 h in vitro; 8 h daily for 3–14 days in vivo) augmented in vitro and in vivo angiogenesis, primarily by stimulating endothelial release of fibroblast growth factor 2 (FGF-2) [Tepper et al., 2004]. In contrast, EMF (10–20 mT, 120 Hz, 10 min daily for 12 days) showed opposite, inhibitory effects on angiogenesis in different animal model systems [Williams et al., 2001]. With regard to the effects of SMF on angiogenesis, a moderate-intensity SMF (200 mT, for 3 h) inhibited prostaglandin E1 (PGE1)- or fetal calf serum-stimulated angiogenesis in chick embryo chorioallantoic membrane in vivo, whereas SMF did not affect the basal pattern of vascularization or chick embryo viability [Ruggiero et al., 2004].

There are several vascular growth factors, such as vascular endothelial growth factor (VEGF) family, FGF, platelet-derived growth factor (PDGF), transforming growth factor β (TGF-β) and prostaglandin E (PGE) family. Of these, VEGF-A has been most carefully and extensively studied for its capacity to develop new blood vessels and plays a predominant role in angiogenesis [Leung et al., 1989; Shweiki et al., 1992] and arteriogenesis [Banai et al., 1994; Couffinhal et al., 1999]. Therefore, in choosing to examine the effects of SMF on endothelial capillary tubule formation in combination with one of the vascular growth factors, we chose VEGF-A.

The present study evaluates the effects of SMF on tubule formation and examines whether the spatial gradient of SMF can accelerate tubule formation. In addition, this investigation is designed to investigate the synergistic effect of SMF and VEGF-A on angiogenesis and/or arteriogenesis.

MATERIALS AND METHODS

Cell Culture

Endothelial capillary tubule formation was evaluated by using an angiogenesis kit (KZ-1000; Kurabo, Osaka, Japan) [Bishop et al., 1999; Donovan et al., 2001; Iba et al., 2002] in which human umbilical vein endothelial cells (HUVEC) and human diploid fibroblasts (HDF) were mixed and seeded into endothelial culture medium in each individual culture well (16 mm diameter) of a 24-well plate made of polystyrene (Falcon, Oxnard, CA, USA) in the optimal condition for the tubule formation. Co-culture of HUVEC and HDF takes advantages of secretion of the necessary matrix components by fibroblasts to act as a scaffold for tubule formation [Bishop et al., 1999]. These co-culture conditions take longer to perform (12–14 days) than the most common in vitro tubule formation assay using HUVEC alone, that is, the Matrigel assay (Matrigel HUVEC tube formation assay) involving a matrix derived from murine tumors, as co-culture assay involves the formation of the extracellular matrix by fibroblasts and then the migration, proliferation, and differentiation of endothelial cells into tubules [Donovan et al., 2001]. Of particular benefit is that the morphology of tubules in the co-culture assay appears more representative of capillary formation relative to the conventional Matrigel assay [Donovan et al., 2001]. The quasi-two-dimensional co-cultured cells were incubated for up to 10 days (240 h) at 37 °C in 5% CO_2 in humidified air and the culture medium was exchanged every 2–3 days. Both cell types proliferated until the culture reached confluence. Endothelial cells became organized among the fibroblasts as corded structures, usually by day 7 [Bishop et al., 1999].

For the experiments on effects of VEGF on tubule formation, the endothelial cells were treated with

recombinant human VEGF-A (R&D Systems, Abingdon, UK) at a concentration of 10 ng/ml. This concentration of VEGF has been used previously to promote tubule formation in co-culture [Bishop et al., 1999; Donovan et al., 2001]. The VEGF-A was added four times to the culture medium from the start of co-culture and the medium was changed with fresh compound in every 2–3 days (0, 3, 6, and 8 day incubation periods) for up to the 10 day (240 h) incubation period.

Static Magnetic Fields (SMF)

The cells of each individual culture well (16 mm in diameter) in a 24-well plate were cultured in the presence or absence of SMF. SMF exposure was carried out using a disc-shaped neodymium magnet (NdFeB, $B_{max} = 320$ mT at the central position on the surface, 16 mm in diameter and 2.5 mm in height, Magna, Tokyo, Japan). A magnet was attached horizontally to the back side of each well and the north (N) side of the magnet was oriented towards the well (Fig. 1A). The maximum magnetic flux density B_{max} was measured to be approximately 120 mT at the bottom center of the well, and the detected field distribution pattern was determined up to 30 mm from the center of the magnet (Fig. 1B) using a gaussmeter (Model 4048, Hall probe A-4048-002; Bell Technologies, Orlando, FL, USA) and a Lab VIEW image analysis software (National Instruments, Austin, TX, USA). Since cells were growing in thin layers at the bottom of the well, the value of B_{max} was obtained on the bottom center of the well at 3 mm above the magnet. This distance is fixed by the space between the magnet and the bottom wall of the well.

As every well on a culture plate was populated with cells, SMF exposure or non-exposure was carried out using a different plate to eliminate the SMF generated by permanent magnets. A 24-well plate had 24 disc magnets applied to each cell-populated well. A similar field distribution pattern was observed within each well. This is because there is adequate spacing between wells (the least distance is 4 mm), eliminating interference of adjacent SMF; 12 wells are shown in Figure 1C. By contrast, non-exposure was performed without magnets. The measured intensity in the non-exposed plate was ~50 μT, which was almost the same as the background geomagnetic field intensity in our laboratory.

The regional spatial magnetic gradient values (G) were calculated on the basis of measured field strengths

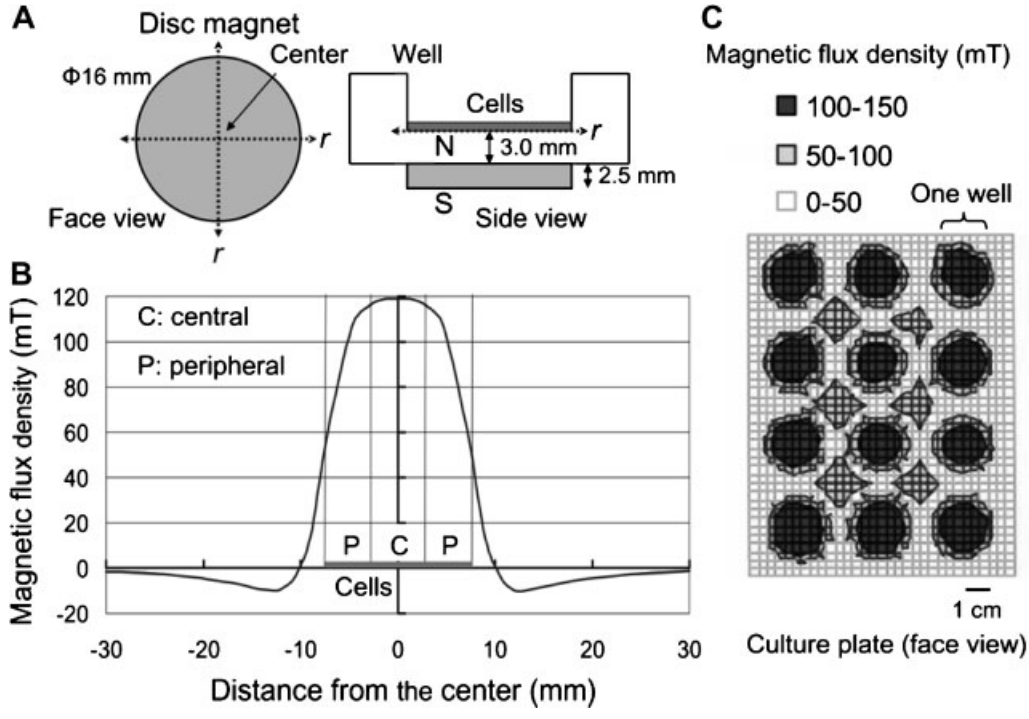

Fig. 1. **A**: A disc-shaped neodymium magnet attached horizontally to the back side of each well. **B**: Spatial distribution of the magnetic flux density on the cells in a well (C: central part [4 mm in radius], P: peripheral part [area 4–8 mm from the center of the well]). **C**: Spatial distribution of the magnetic flux density on the cells in 12 wells. The smallest distance between cell-populated wells is 4 mm. There is a similar field distribution pattern within each well.

and were estimated in cylindrical coordinates (r, θ, z) using Equation (1):

$$|G| = \sqrt{\left(\frac{\partial B_r}{\partial r}\right)^2 + \left[\left(\frac{1}{r}\right)\left(\frac{\partial B_\theta}{\partial \theta}\right)\right]^2 + \left(\frac{\partial B_z}{\partial z}\right)^2} \quad (1)$$

where axial symmetry gives $\partial B_\theta/\partial\theta = 0$ and the thin layers (less than 30 μm-thick) of cells gives $\partial B_z/\partial z \cong 0$, and consequently $|G| = \partial B_r/\partial r$.

The calculations indicate that the maximum spatial magnetic gradient value (G_{max}) within a well is 21 mT/mm at the bottom peripheral part of the well (Fig. 2). The magnetic gradient values fall to near 0 mT/mm at the bottom center of the well (Fig. 2).

Experimental Procedures

Four experimental protocols were performed: (1) non-exposure alone (control); (2) SMF exposure alone; (3) non-exposure with VEGF-A; (4) SMF exposure with VEGF-A. The SMF or non-exposure was carried out for up to 10 days. Photomicrographs of tubule cells immunostained with an anti-CD31 (PECAM-1) antibody were analyzed after culture at 37 °C for 4, 7, and 10 days. Each plate of cells with or without magnets was always placed apart from others on the same shelf in a tissue culture incubator where the ambient 60 Hz magnetic field is under 1 μT.

Immunostaining

On days 4, 7, and 10, cells were fixed at room temperature in 70% ice-cold ethanol stored at −20 °C. Platelet endothelial cell adhesion molecule-1 (PECAM-1), also called CD31 (clone JC70; Dako, Denmark), a 100 kDa glycoprotein that participates in the adhesion between platelets and endothelial cells [Newman et al., 1990]. The PECAM-1 (CD31) was visualized as a pan-endothelial marker [Parums et al., 1990] by staining with a tubule staining kit (Kurabo, Osaka, Japan) [Bishop et al., 1999; Donovan et al., 2001; Iba et al., 2002] including the primary antibody, a monoclonal mouse anti-human PECAM-1 antibody and the secondary antibody, a polyclonal goat anti-mouse IgG alkaline phosphatase-conjugated antibody. Briefly, tubules were visualized by staining for PECAM-1 by washing cells with PBS containing 1% BSA and incubated with the primary antibody for 1 h at 37 °C. Cells were washed and incubated with the secondary antibody for 1 h at 37 °C. Color detection was performed using 5-bromo-4-chloro-3-indolyl-phosphate/nitro blue tetrazolium (BCIP/NBT; Sigma, St. Louis, MO) as substrate (purple precipitate with light microscopy) according to the manufacturer's recommendation.

Image Analysis

The whole area of each well was immunostained with an anti-CD31 antibody and was captured with a digital camera (C-5050 Zoom; Olympus, Tokyo) and saved as TIFF images. The photomicrographs were quantified by using Scion software (Scion Image; Scion, Frederick, MD, USA). Images of tubule cells were imported into Scion Image and converted to binary format. The binary threshold function was adjusted to obtain the best contrast of tubules with background and

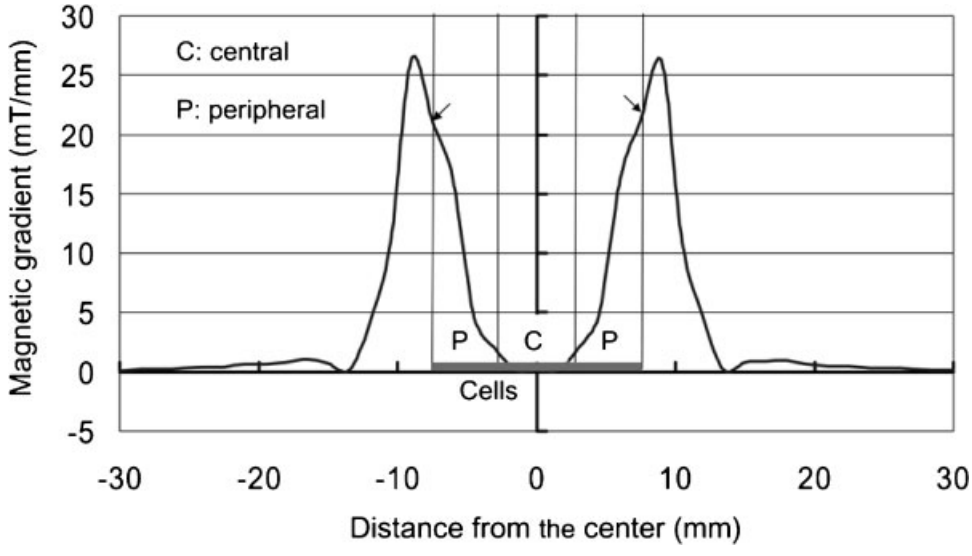

Fig. 2. The magnetic gradient values within a well peak at 21 mT/mm, as shown by arrows, at the bottom peripheral part of the well and fall near to 0 mT/mm at the bottom center of the well (C, central part [4 mm in radius]; P, peripheral part [area 4–8 mm from the center of the well]).

was set constant for all the groups. The luminal area was calculated as the total number of pixels in the threshold images. The unit of the area density is expressed as area rate (luminal area/whole area; %).

As parameters of tubule formation, the mean values of the area density and the length of tubules as well as the number of bifurcations were determined and compared between the groups. The measurement area of each well (8 mm in radius) was divided into two parts: the central part (4 mm in radius) and peripheral part (area 4–8 mm from the center of the well), that is, the whole area without the central area.

Statistical Analysis

Two-way analysis of variance (ANOVA) was used to evaluate the effects of exposure (exposure vs. non-exposure) and gradient (center vs. peripheral portion) and all combinations there of using the SAS GLM procedure (SAS 9.1; SAS Institute, Cary, NC, USA). Dunnett's multiple comparison test and Wilcoxon rank sum test were used as post hoc tests if significant different means were detected. All values are expressed as mean ± SEM. A difference of $P < .05$ was considered statistically significant.

RESULTS

Tubule Formation in Baseline Control

To assess the distribution of the intact tubule formation in wells, the mean values of the area density, the length of tubules and the number of bifurcations in controls were compared between the peripheral and central part of the wells. All the parameters of tubule formation in the peripheral part were two to four times higher than those in the central part. During the incubation period investigated, the ratios of differences in the area density between peripheral/central (P/C) decreased in time: day 4, 3.77; day 7, 3.02; day 10, 2.83. Those in the length were relatively stable: day 4, 2.08; day 7, 2.29; day 10, 2.29 while, those in the number of bifurcations increased: day 4, 1.81; day 7, 2.48; day 10, 2.73 (Tables 1–3).

Effects of SMF Alone on Tubule Formation

After a 10 day incubation, SMF alone induced a significant increase in the mean values of the area density and the length of tubules in the peripheral part of the wells (SMF [P]), compared with the corresponding control group (CTL [P]), whereas SMF by itself did not induce any significant changes in those values in the central part of the wells (SMF [C] vs. CTL [C]) (Tables 1–3, Figs. 3, 5 and 6). On day 10, the ratios of peripheral/central (P/C) differences in the area density were higher in SMF (3.28) relative to CTL (2.83) (Table 3). On day 10, the mean values of the area density (%) and the length of tubules (mm/mm^2) are 6.95% and 0.49 mm/mm^2 in SMF [P] and 5.07% and 0.39 mm/mm^2 in CTL [P], respectively (Table 3). The mean values of the area density and the length of tubules in the SMF-exposed peripheral part of the wells (SMF [P]) were significantly higher than those in the SMF-exposed central part of the wells (SMF [C]) following the 4–10 day incubation periods (Tables 1–3). However, SMF did not induce any significant changes in the mean values of the number of bifurcations in any part of the wells, compared with the corresponding control group (SMF [C] and [P] vs.

TABLE 1. Parameters of Tubule Formation Measured in the Central and Peripheral Area of Each Well After Culture at 37 °C for 4 Days

Parameter [part] (unit)	CTL ($n = 10$)	SMF ($n = 10$)	VG ($n = 10$)	SMF + VG ($n = 10$)
Area density [C] (%)	0.75 ± 0.12	0.82 ± 0.09	1.15 ± 0.09	1.20 ± 0.05
Area density [P] (%)	$2.83 \pm 0.15^{\dagger,b}$	$3.08 \pm 0.35^{\dagger,b}$	$3.85 \pm 0.20^{*,a,\dagger,b}$	$4.16 \pm 0.36^{\dagger,b}$
Area density [P/C] (ratio)	3.77	3.75	3.35	3.47
Length [C] (mm/mm^2)	0.12 ± 0.01	0.13 ± 0.01	0.16 ± 0.02	0.18 ± 0.02
Length [P] (mm/mm^2)	$0.25 \pm 0.02^{\dagger,b}$	$0.27 \pm 0.02^{\dagger,b}$	$0.38 \pm 0.05^{**,a,\dagger,b}$	$0.41 \pm 0.04^{\dagger,b}$
Length [P/C] (ratio)	2.08	2.08	2.38	2.28
No. of bifurcations [C] (points/mm^2)	0.16 ± 0.02	0.17 ± 0.02	0.19 ± 0.02	0.21 ± 0.02
No. of bifurcations [P] (points/mm^2)	$0.29 \pm 0.03^{\dagger,b}$	$0.31 \pm 0.03^{\dagger,b}$	$0.39 \pm 0.03^{*,a,\dagger,b}$	$0.43 \pm 0.03^{\dagger,b}$
No. of bifurcations [P/C] (ratio)	1.81	1.82	2.05	2.05

CTL, control; SMF, static magnetic field; VG, VEGF-A; C, central area; P, peripheral area. Values represent mean ± SEM. n, no. of samples measured per group.
$^*P < .01$; $^{**}P < .001$; VG versus the corresponding CTL.
$^{\dagger}P < .001$; C versus the corresponding P.
[a]Significantly higher than the CTL.
[b]Significantly higher than the C.

TABLE 2. Parameters of Tubule Formation Measured in the Central and Peripheral Area of Each Well After Culture at 37 °C for 7 Days

Parameter [part] (unit)	CTL ($n=10$)	SMF ($n=10$)	VG ($n=10$)	SMF + VG ($n=10$)
Area density [C] (%)	1.40 ± 0.15	1.66 ± 0.12	$2.76 \pm 0.14^{*,a}$	2.97 ± 0.18
Area density [P] (%)	$4.23 \pm 0.25^{\dagger,b}$	$5.14 \pm 0.42^{\dagger,b}$	$5.93 \pm 0.47^{*,a,\dagger,b}$	$6.86 \pm 0.32^{\dagger,b}$
Area density [P/C] (ratio)	3.02	3.10	2.15	2.31
Length [C] (mm/mm^2)	0.14 ± 0.02	0.17 ± 0.02	$0.28 \pm 0.03^{*,a}$	0.30 ± 0.03
Length [P] (mm/mm^2)	$0.32 \pm 0.03^{\dagger,b}$	$0.39 \pm 0.03^{\dagger,b}$	$0.56 \pm 0.03^{*,a,\dagger,b}$	$0.61 \pm 0.04^{\dagger,b}$
Length [P/C] (ratio)	2.29	2.29	2.00	2.03
No. of bifurcations [C] (points/mm^2)	0.21 ± 0.02	0.23 ± 0.02	$0.32 \pm 0.03^{*,a}$	0.33 ± 0.03
No. of bifurcations [P] (points/mm^2)	$0.52 \pm 0.05^{\dagger,b}$	$0.55 \pm 0.05^{\dagger,b}$	$0.75 \pm 0.07^{*,a,\dagger,b}$	$0.78 \pm 0.07^{\dagger,b}$
No. of bifurcations [P/C] (ratio)	2.48	2.39	2.34	2.36

CTL, control; SMF, static magnetic field; VG, VEGF-A; C, central area; P, peripheral area. Values represent mean ± SEM. n, no. of samples measured per group.
*$P < .001$; VG versus the corresponding CTL.
†$P < .001$; C versus the corresponding P.
[a]Significantly higher than the CTL.
[b]Significantly higher than the C.

CTL [C] and [P]) (Tables 1–3, Figs. 3 and 7). The tubule cells in the wells had elongated, spindle-like shapes and the direction of cell elongation was random, irrespective of the presence and direction of SMF (Fig. 3).

Effects of VEGF-A Alone on Tubule Formation

VEGF-A significantly promoted all the parameters of tubule formation in the peripheral part of the wells (VG [P]) following the 4–10 day incubation periods, compared with the corresponding control group (CTL [P]) (Tables 1–3, Figs. 4–7). In addition, in the central part of the wells, VEGF-A significantly increased all the parameters of tubule formation (VG [C]) following the 7–10 day incubation periods, compared with the corresponding control group (CTL [C]; Tables 1–3, Figs. 4–7). In particular, the ratios of peripheral/central (P/C) differences in the area density were lower in VG relative to CTL during the 7–10 day incubation periods (Tables 2 and 3).

Synergistic Effects of SMF and VEGF-A on Tubule Formation

With regard to the combined effects of SMF and VEGF-A on tubule formation, SMF significantly promoted the VEGF-A-increased mean values of the area density and the length of tubules in the peripheral

TABLE 3. Parameters of Tubule Formation Measured in the Central and Peripheral Area of Each Well After Culture at 37 °C for 10 Days

Parameter [part] (unit)	CTL ($n=25$)	SMF ($n=25$)	VG ($n=25$)	SMF + VG ($n=25$)
Area density [C] (%)	1.79 ± 0.21	2.12 ± 0.30	$3.71 \pm 0.27^{*,a}$	4.01 ± 0.29
Area density [P] (%)	$5.07 \pm 0.42^{\dagger,b}$	$6.95 \pm 0.46^{\dagger,b,\ddagger,c}$	$7.84 \pm 0.44^{*,a,\dagger,b}$	$9.75 \pm 0.40^{\dagger,b,\ddagger,c}$
Area density [P/C] (ratio)	2.83	3.28	2.11	2.43
Length [C] (mm/mm^2)	0.17 ± 0.02	0.20 ± 0.02	$0.33 \pm 0.02^{*,a}$	0.36 ± 0.02
Length [P] (mm/mm^2)	$0.39 \pm 0.02^{\dagger,b}$	$0.49 \pm 0.02^{\dagger,b,\ddagger,c}$	$0.69 \pm 0.04^{*,a,\dagger,b}$	$0.80 \pm 0.05^{\dagger,b,\ddagger,c}$
Length [P/C] (ratio)	2.29	2.45	2.09	2.22
No. of bifurcations [C] (points/mm^2)	0.22 ± 0.02	0.25 ± 0.03	$0.38 \pm 0.02^{*,a}$	0.40 ± 0.02
No. of bifurcations [P] (points/mm^2)	$0.60 \pm 0.03^{\dagger,b}$	$0.63 \pm 0.03^{\dagger,b}$	$0.93 \pm 0.05^{*,a,\dagger,b}$	$0.97 \pm 0.05^{\dagger,b}$
No. of bifurcations [P/C] (ratio)	2.73	2.52	2.45	2.43

CTL, control; SMF, static magnetic field; VG, VEGF-A; C, central area; P, peripheral area. Values represent mean ± SEM. n, no. of samples measured per group.
*$P < .001$; VG versus the corresponding CTL.
†$P < .001$; C versus the corresponding P.
‡$P < .01$; SMF versus the corresponding CTL, SMF + VG versus the corresponding VG.
[a]Significantly higher than the CTL.
[b]Significantly higher than the C.
[c]Significantly higher than the CTL or VG.

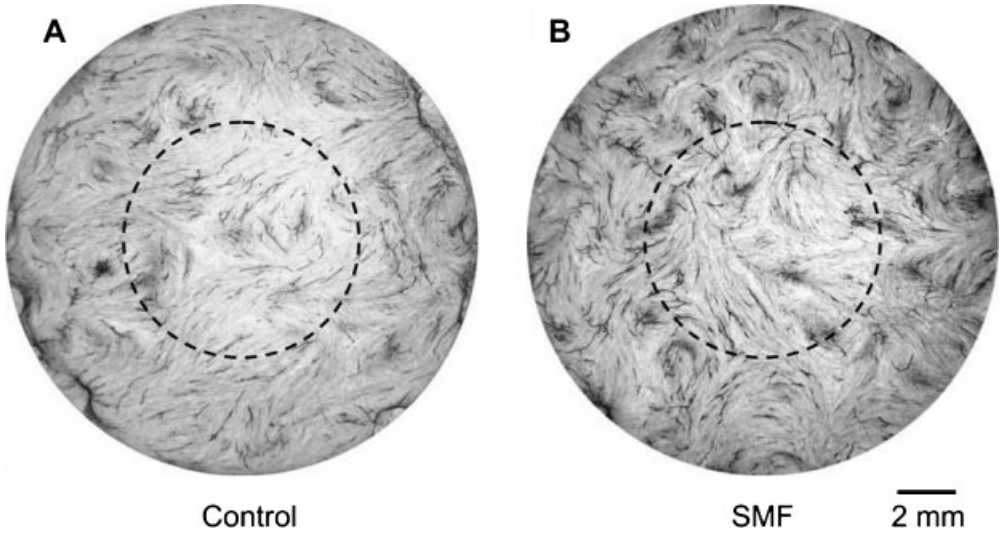

Fig. 3. Day 10 of co-culture of human umbilical vein endothelial cells (HUVEC) and human diploid fibroblasts (HDF) in the central part (inside the dotted line) and the peripheral part (outside the dotted line) of a well. **A**: Day 10 culture without exposure to SMF (control), showing microvessel-like structures in confluent quasi-monolayers. **B**: Day 10 culture with continuous exposure to SMF for 10 days, showing SMF induced increases in the density and the length of tubules specifically in the peripheral part of a culture well (see also Table 3). The direction of cell elongation was random, irrespective of the presence and direction of SMF.

part of the wells (SMF + VG [P]) following the 10 day incubation period, compared with VEGF-A treatment alone (VG [P]) (Tables 1–3, Figs. 4–7). In the central part of the wells, however, SMF did not induce any significant changes in any parameter of tubule formation (SMF + VG [C]) during the 4–10 day incubation periods, compared with VEGF-A treatment alone (VG [C]) (Tables 1–3, Figs. 4–7). In particular, on day 10, the ratios of peripheral/central (P/C) differences in the area density were higher in the combination of SMF and VEGF-A treatment (SMF + VG, 2.43) relative to VEGF-A treatment alone (VG, 2.11; Table 3).

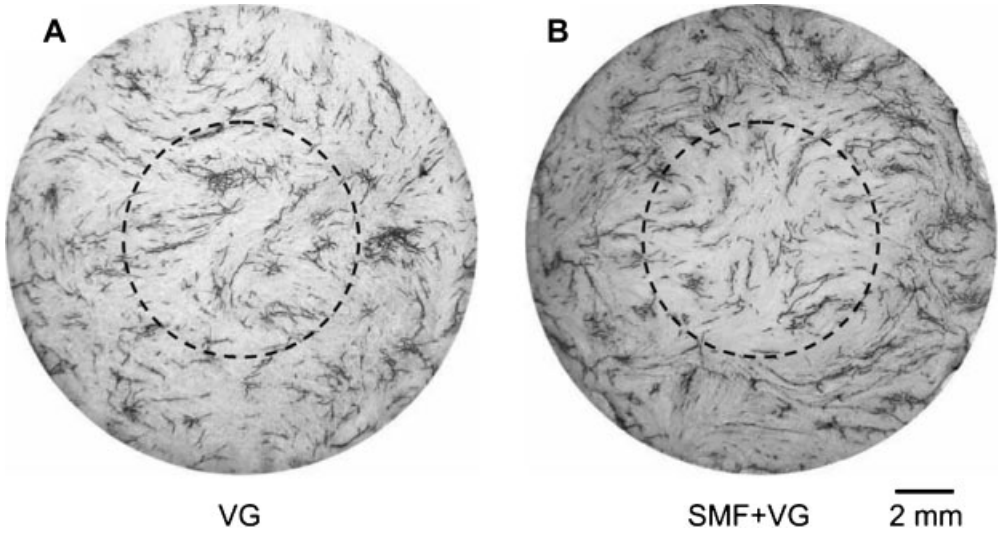

Fig. 4. Day 10 of co-culture of HUVEC and HDF, in which VEGF-A (10 ng/ml) was present from day 0, in the central part (inside the dotted line) and the peripheral part (outside the dotted line) of a well. **A**: Day 10 culture without exposure to SMF, showing VEGF-A-induced increases in the density and the length of tubules as well as the number of bifurcations (see also Table 3). **B**: Day 10 culture with continuous exposure to SMF for 10 days, showing synergistic effects of SMF on VEGF-A-enhanced tubule formation in terms of the density and the length of tubules (see also Table 3).

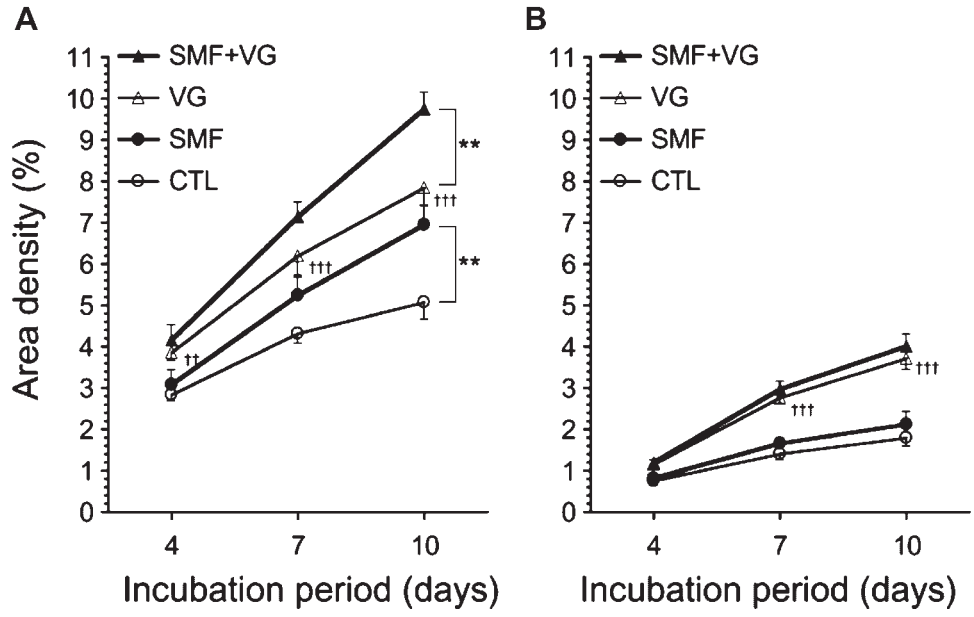

Fig. 5. Temporal development of the area density in tubule formation. **A**: Peripheral area. **B**: Central area. SMF + VG, SMF exposure with VEGF-A; VG, control exposure with VEGF-A; CTL, control. Values represent mean ± SEM ($n = 10$ in each group after 4- and 7-day incubation periods, $n = 25$ in each group after a 10-day incubation period). $^{\dagger\dagger}P < .01$, $^{\dagger\dagger\dagger}P < .001$; VG versus the corresponding CTL. $^{**}P < .01$; SMF versus the corresponding CTL, SMF + VG versus the corresponding VG.

DISCUSSION

The P/C differences in all the parameters of tubule formation were seen in all experimental conditions, including baseline controls, throughout the experimental period of 10 days: in particular, the SMF had its largest apparent effects on the tubule formation in the peripheral areas on day 10. These dense peripheral changes of the tubule formation manifested in co-culture of HUVEC and HDF as highly concentrated filaments. As for the reason of P/C differences, the rounded bottom edge or corner walls of wells might act as a physical scaffold for tubule formation: these geographical effects are called ''corner effects'' (they would not be technical errors in incubation).

To evaluate the influences of SMF on the tubule formation, it is important to distinguish the effects of SMF on between angiogenesis and arteriogenesis. Angiogenesis results in an increase in the number of capillaries [Yang et al., 1994; Wagner, 2000] and occurs by the processes of sprouting (a capillary branch emerges out from an existing capillary) and intussusception (a single capillary splits into two capillaries by the formation of a longitudinal divide on the luminal side of the capillary) [Prior et al., 2004]. On the other hand, arteriogenesis involves the enlargement and elongation of existing blood vessels and is accomplished by both endothelial and smooth muscle cell proliferation [van Royen et al., 2001]. Briefly, an increase in angiogenesis affects the number of bifurcations (new capillaries sprouting off from existing vessels and bridging between existing blood vessels), whereas an increase in density and/or length without a corresponding increase in the number of bifurcations would generally suggest the enlargement and elongation of existing blood vessels, that is, arteriogenesis.

The present study demonstrates that a moderate-intensity SMF with spatial gradient alone significantly promoted arteriogenic parameters, the area density and the length of tubules in the peripheral part of the culture wells, whereas the SMF by itself did not cause significant changes in an angiogenic parameter, the number of bifurcations, in any part of the wells. While VEGF-A is the most ubiquitous mediator of both angiogenesis and arteriogenesis, the synergistic effects of SMF and VEGF-A on arteriogenesis but not angiogenesis appear to be found exclusively in the peripheral part of the wells. Therefore, these results suggest that SMF leads mainly to augmentation of arteriogenesis in the peripheral part of the wells, where the spatial gradient increases relative to the central part. The gradient portion of SMF could be responsible for the observed biological responses. These findings might assert the same effects of inhomogeneous SMF on

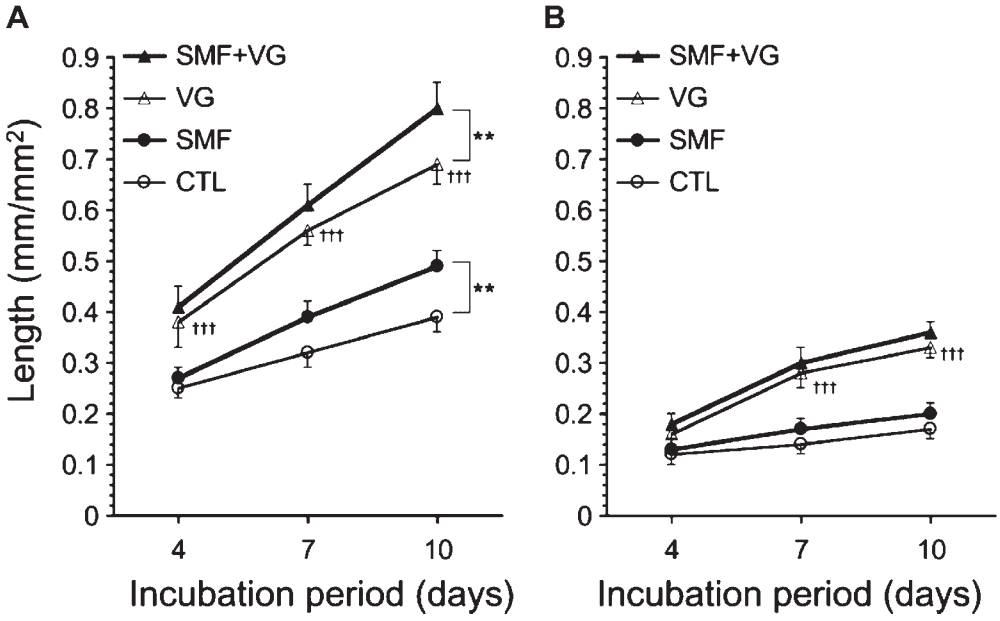

Fig. 6. Temporal development of the tubule length. **A**: Peripheral area. **B**: Central area. SMF + VG, SMF exposure with VEGF-A; VG, control exposure with VEGF-A; CTL, control. Values represent mean ± SEM ($n = 10$ in each group after 4- and 7-day incubation periods, $n = 25$ in each group after a 10-day incubation period). $^{\dagger\dagger\dagger}P < .001$; VG versus the corresponding CTL. $^{**}P < .01$; SMF versus the corresponding CTL, SMF + VG versus the corresponding VG.

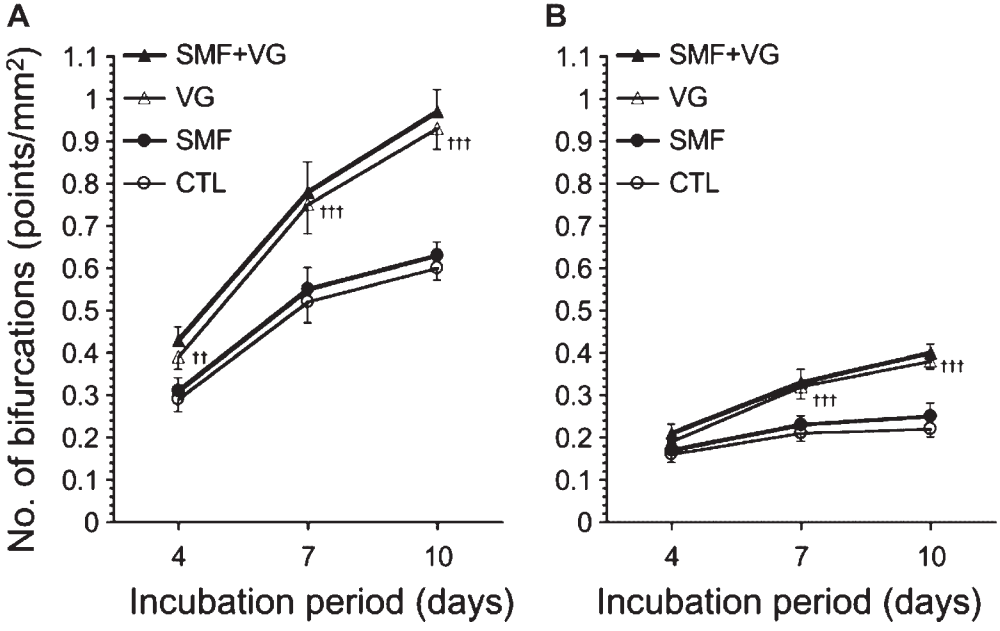

Fig. 7. Temporal development of the number of bifurcations in tubule formation. **A**: Peripheral area. **B**: Central area. SMF + VG, SMF exposure with VEGF-A; VG, control exposure with VEGF-A; CTL, control. Values represent mean ± SEM ($n = 10$ in each group after 4- and 7-day incubation periods, $n = 25$ in each group after a 10-day incubation period). $^{\dagger\dagger}P < .01$, $^{\dagger\dagger\dagger}P < .001$; VG versus the corresponding CTL.

action potential generation [Cavopol et al., 1995; McLean et al., 1995] and myosin phosphorylation [Engström et al., 2002].

We have been investigating the effects of SMF on bone fracture healing in vivo and the results revealed that SMF exposure (B_{max} 180 mT, for 12 weeks) significantly prevented the reduction in bone mineral density (BMD) of rats caused by surgical invasion or implantation of a small piece of tapered magnetic rod (6 mm in length, 1.5 mm in maximum diameter, 45 mg in weight) to the femur [Yan et al., 1998]. In addition, the enhanced effect of SMF exposure (B_{max} 180 mT, for 3 weeks) on BMD of rats was observed in rats with reduced blood flow (ischemia) created by surgically ligating rat arteries, and suggested that it might be due to the improved blood circulation [Xu et al., 2001]. Based on the results obtained in this study showing the enhanced effects of SMF by itself on tubule formation, the ability of SMF to augment the bone repair process might be, at least in part, related to the increased arteriogenesis, which could result in promotion of bone formation by improving blood circulation.

Other studies revealed that SMF values in the range of $B_{max} = 8-180$ mT can promote bone fracture healing or bone formation in vitro [Yamamoto et al., 2003; Yuge et al., 2003; Shimizu et al., 2004; Huang et al., 2006] and in vivo [Bruce et al., 1987; Mevissen et al., 1994; Darendeliler et al., 1997; Qin et al., 2004]. In particular, SMF in the range of 100–180 mT, average 160 mT, for 8–20 days, are able to affect osteogenesis by promoting osteoblast differentiation and/or activation via the increased calcium content, alkaline phosphatase and osteocalcin, without affecting osteoblast proliferation [Yamamoto et al., 2003]. In addition, SMF ($B_{max} = 30$ or 80 mT, for 24 h) can also promote osteogenesis by enhancing bone sialoprotein (BSP) expression through fibroblast growth factor-2 (FGF-2) response element and pituitary-specific transcription factor-1 motif [Shimizu et al., 2004].

In addition to measuring the intensities applied, determining the spatial gradient properties of SMF is important to explore the mechanism(s) responsible for inducing the effects of SMF on biological systems [Engström et al., 2005]. In most of these studies investigating the effects of SMF, however, the values of the spatial gradients of SMF have not been clearly determined or documented. In our present study, the maximum gradient value of SMF applied to intact or VEGF-A-stimulated vascular endothelial cells was calculated to be 21 mT/mm, which caused significant increase in arteriogenetic parameters in tubule formation. Moreover, as the magnetic forces are proportional to magnetic flux densities × spatial gradients, the magnetic force applied should be considered as a mechanism of SMF on cellular mechanotransduction or mechanical stress. For example, with regard to SMF-induced cellular mechanotransduction, it is shown that a moderate-intensity magnetic force, for example, 50 mT-induced force gradually accelerated osteoblast differentiation from 10 min to 21 days, primarily due to the activation of p38 phosphorylation (the regional magnetic force was not described) [Yuge et al., 2003].

The regional magnetic force F_m on 1 cm^3 of materials oriented along the r-axis is estimated according to Equation (2).

$$F_m = |B_r|\,|G_r|\left|\frac{\chi_v}{\mu_0}\right| \tag{2}$$

where B_r = regional magnetic flux density oriented along the $+r$-direction; G_r = regional magnetic gradient oriented along the $+r$-axis; χ_v = volumetric magnetic susceptibility; μ_0 = magnetic permeability of free space ($\cong 1$ for air in cgs units). Almost all human tissues have diamagnetic anisotropic properties and the magnetic susceptibilities of most tissues appear to be in a narrow range of about ±20% from that of water, which is -0.72×10^{-6} cgs emu/cm^3 at physiological temperature (37 °C or 310 K) [Schenck, 1996].

The vector of the magnetic forces is proportional to the calculated values of $B_r \times G_r$. In the present study, the calculated value of $B_r \times G_r$ is peaked at the peripheral edge of the well, at which the value of B_r (0.052 T) × G_r (= G_{max} 21 T/m) is 1.09 T^2/m. Using Equation (2), the calculated maximum value of the repelling magnetic force on the diamagnetic anisotropic biomaterials in the peripheral part of the wells is 0.8 μN/cm^3. This diamagnetic force value would be considered to be equivalent or higher than those of other studies performed to investigate the modulating effects of relatively uniform SMF on in vivo angiogenesis [Ruggiero et al., 2004] or in vitro osteogenesis [Yamamoto et al., 2003; Yuge et al., 2003; Shimizu et al., 2004; Huang et al., 2006], whereas the magnetic force value did not induce cell orientation in relation to the magnetic direction. The baseline P/C differences in the co-culture cells, probably due to corner effects, might be enhanced by the magnetic force acting as a mechanical stress.

In our experiment, the controls were not a true sham in that a similar metal material disc was not used as a dummy magnet. Each plate of cells with or without magnets was always placed apart on the same shelf made of stainless steel in a tissue culture incubator. As a measurable physical characteristic, the temperature (37 °C during incubation) inside the wells of magnet groups (SMF or SMF + VG) did not differ from the

controls and, irrespective of the presence or absence of magnets, uniform and stable distribution of temperature inside each individual well was observed in every experimental group using thermometer probes (data not shown). These results suggest that the mere presence of the metal of the magnet had no thermal effects on each cell in any experimental group, at least not through radiant heat transport.

By characterizing the parameters and factors of the applied SMF, the effects of SMF on promoting normal arteriogenesis in conjunction with osteogenesis could be exploited to improve blood circulation and promote bone fracture healing or prevent osteoporosis. The mechanisms underlying these effects of the magnetic forces produced by moderate-intensity gradient SMF need to be clarified.

CONCLUSIONS

It was concluded that the application of a moderate-intensity gradient SMF to intact or VEGF-A stimulated vascular endothelial cells could lead mainly to promote or enhance the arteriogenesis in the peripheral part of the wells, where the spatial gradient increased relative to the central part, without cell orientation in relation to the magnetic direction. The effects of SMF on the VEGF-A-enhanced tubule formation appear to be synergistic or additive in arteriogenesis but not in angiogenesis.

ACKNOWLEDGMENTS

We thank Dr. Kouji Takano for measurement and analysis of spatial distribution of magnetic flux density in the magnet.

REFERENCES

Arbiser JL. 1996. Angiogenesis and the skin: A primer. J Am Acad Dermatol 34:486–497.

Banai S, Jaklitsch MT, Shou M, Lazarous DF, Scheinowitz M, Biro S, Epstein SE, Unger EF. 1994. Angiogenic-induced enhancement of collateral blood flow to ischemic myocardium by vascular endothelial growth factor in dogs. Circulation 89:2183–2189.

Battegay EJ. 1995. Angiogenesis: Mechanistic insights, neovascular diseases, and therapeutic prospects. J Mol Med 73: 333–346.

Bishop ET, Bell GT, Bloor S, Broom IJ, Hendry NF, Wheatley DN. 1999. An in vitro model of angiogenesis: Basic features. Angiogenesis 3:335–344.

Boucher Y, Leunig M, Jain RK. 1996. Tumor angiogenesis and interstitial hypertension. Cancer Res 56:4264–4266.

Bruce GK, Howlett CR, Huckstep RL. 1987. Effect of a static magnetic field on fracture healing in a rabbit radius. Preliminary results. Clin Orthop Relat Res 222:300–306.

Carmeliet P, Jain RK. 2000. Angiogenesis in cancer and other diseases. Nature 407:249–257.

Cavopol AV, Wamil AW, Holcomb RR, McLean MJ. 1995. Measurement and analysis of static magnetic fields that block action potentials in cultured neurons. Bioelectromagnetics 16:197–206.

Couffinhal T, Silver M, Kearney M, Sullivan A, Witzenbichler B, Magner M, Annex B, Peters K, Isner JM. 1999. Impaired collateral vessel development associated with reduced expression of vascular endothelial growth factor in ApoE−/− mice. Circulation 99:3188–3198.

Darendeliler MA, Darendeliler A, Sinclair PM. 1997. Effects of static magnetic and pulsed electromagnetic fields on bone healing. Int J Adult Orthodon Orthognath Surg 12: 43–53.

Donovan D, Brown NJ, Bishop ET, Lewis CE. 2001. Comparison of three in vitro human 'angiogenesis' assays with capillaries formed in vivo. Angiogenesis 4:113–121.

Donski PK, Carwell GR, Sharzer LA. 1979. Growth in revascularized bone grafts in young puppies. Plast Reconstr Surg 64: 239–243.

Engström S, Markov MS, McLean MJ, Holcomb RR, Markov JM. 2002. Effects of non-uniform static magnetic fields on the rate of myosin phosphorylation. Bioelectromagnetics 23: 475–479.

Engström S, Markov MS, McLean MJ, Jones RA, Holcomb RR. 2005. Devices for gradient static magnetic field exposure. Bioelectromagnetics 26:336–340.

Folkman J. 1990. How the field of controlled-release technology began, and its central role in the development of angiogenesis research. Biomaterials 11:615–618.

Folkman J. 1992. The role of angiogenesis in tumor growth. Semin Cancer Biol 3:65–71.

Folkman J, Ingber D. 1992. Inhibition of angiogenesis. Semin Cancer Biol 3 :89–96.

Fukumura D, Xavier R, Sugiura T, Chen Y, Park EC, Lu N, Selig M, Nielsen G, Taksir T, Jain RK, Seed B. 1998. Tumor induction of VEGF promoter activity in stromal cells. Cell 94:715–725.

Fukumura D, Gohongi T, Kadambi A, Izumi Y, Ang J, Yun CO, Buerk DG, Huang PL, Jain RK. 2001. Predominant role of endothelial nitric oxide synthase in vascular endothelial growth factor-induced angiogenesis and vascular permeability. Proc Natl Acad Sci USA 98:2604–2609.

Gmitrov J, Ohkubo C. 2002a. Artificial static and geomagnetic field interrelated impact on cardiovascular regulation. Bioelectromagnetics 23:329–338.

Gmitrov J, Ohkubo C. 2002b. Verapamil protective effect on natural and artificial magnetic field cardiovascular impact. Bioelectromagnetics 23:531–541.

Gmitrov J, Ohkubo C, Okano H. 2002. Effect of 0.25 T static magnetic field on microcirculation in rabbits. Bioelectromagnetics 23:224–229.

Huang HM, Lee SY, Yao WC, Lin CT, Yeh CY. 2006. Static magnetic fields up-regulate osteoblast maturity by affecting local differentiation factors. Clin Orthop Relat Res *published online*: Jan 26.

Iba O, Matsubara H, Nozawa Y, Fujiyama S, Amano K, Mori Y, Kojima H, Iwasaka T. 2002. Angiogenesis by implantation of peripheral blood mononuclear cells and platelets into ischemic limbs. Circulation 106:2019–2025.

Ingber D, Fujita T, Kishimoto S, Sudo K, Kanamaru T, Brem H, Folkman J. 1990. Synthetic analogues of fumagillin that

inhibit angiogenesis and suppress tumour growth. Nature 348:555–557.
Jain RK. 2002. Tumor angiogenesis and accessibility: Role of vascular endothelial growth factor. Semin Oncol 29:3–9.
Jain RK. 2005. Normalization of tumor vasculature: An emerging concept in antiangiogenic therapy. Science 307:58–62.
Jain RK, Koenig GC, Dellian M, Fukumura D, Munn LL, Melder RJ. 1996. Leukocyte-endothelial adhesion and angiogenesis in tumors. Cancer Metastasis Rev 15:195–204.
Leung DW, Cachianes G, Kuang WJ, Goeddel DV, Ferrara N. 1989. Vascular endothelial growth factor is a secreted angiogenic mitogen. Science 246:1306–1309.
Leunig M, Yuan F, Menger MD, Boucher Y, Goetz AE, Messmer K, Jain RK. 1992. Angiogenesis, microvascular architecture, microhemodynamics, and interstitial fluid pressure during early growth of human adenocarcinoma LS174T in SCID mice. Cancer Res 52:6553–6560.
McLean MJ, Holcomb RR, Wamil AW, Pickett JD, Cavopol AV. 1995. Blockade of sensory neuron action potentials by a static magnetic field in the 10 mT range. Bioelectromagnetics 16:20–32.
Melder RJ, Koenig GC, Witwer BP, Safabakhsh N, Munn LL, Jain RK. 1996. During angiogenesis, vascular endothelial growth factor and basic fibroblast growth factor regulate natural killer cell adhesion to tumor endothelium. Nat Med 2:992–997.
Mevissen M, Buntenkotter S, Loscher W. 1994. Effects of static and time-varying (50-Hz) magnetic fields on reproduction and fetal development in rats. Teratology 50:229–237.
Morris C, Skalak T. 2005. Static magnetic fields alter arteriolar tone in vivo. Bioelectromagnetics 26:1–9.
Newman PJ, Berndt MC, Gorski J. 1990. PECAM-1 (CD31) cloning and relation to adhesion molecules of the immunoglobulin gene superfamily. Science 247:1219–1222.
Ohkubo C, Xu S. 1997. Acute effects of static magnetic fields on cutaneous microcirculation in rabbits. In Vivo 11:221–225.
Okano H, Ohkubo C. 2001. Modulatory effects of static magnetic fields on blood pressure in rabbits. Bioelectromagnetics 22:408–418.
Okano H, Ohkubo C. 2003a. Anti-pressor effects of whole-body exposure to static magnetic field on pharmacologically induced hypertension in conscious rabbits. Bioelectromagnetics 24:139–147.
Okano H, Ohkubo C. 2003b. Effects of static magnetic fields on plasma levels of angiotensin II and aldosterone associated with arterial blood pressure in genetically hypertensive rats. Bioelectromagnetics 24:403–412.
Okano H, Ohkubo C. 2005a. Effects of neck exposure to 5.5 mT static magnetic field on pharmacologically modulated blood pressure in conscious rabbits. Bioelectromagnetics 26:469–480.
Okano H, Ohkubo C. 2005b. Exposure to a moderate-intensity static magnetic field enhances the hypotensive effect of a calcium channel blocker in spontaneously hypertensive rats. Bioelectromagnetics 26:611–623.
Okano H, Gmitrov J, Ohkubo C. 1999. Biphasic effects of static magnetic fields on cutaneous microcirculation in rabbits. Bioelectromagnetics 20:161–171.
Okano H, Masuda H, Ohkubo C. 2005a. Effects of 25 mT static magnetic field on blood pressure in reserpine-induced hypotensive Wistar-Kyoto rats. Bioelectromagnetics 26: 36–48.
Okano H, Masuda H, Ohkubo C. 2005b. Decreased plasma levels of nitric oxide metabolites, angiotensin II and aldosterone in spontaneously hypertensive rats exposed to 5 mT static magnetic field. Bioelectromagnetics 26:161–172.
Parums DV, Cordell JL, Micklem K, Heryet AR, Gatter KC, Mason DY. 1990. JC70: A new monoclonal antibody that detects vascular endothelium associated antigen on routinely processed tissue sections. J Clin Pathol 43:752–757.
Prior BM, Yang HT, Terjung RL. 2004. What makes vessels grow with exercise training? J Appl Physiol 97:1119–1128.
Qin K, Qiu LH, Zhong M, Wang ZY. 2004. The effect of static magnetic field on bone morphogenetic protein-2 in periodontal membrane of the rat. Shanghai Kou Qiang Yi Xue 13: 275–277.
Reynolds LP, Redmer DA. 1998. Expression of the angiogenic factors, basic fibroblast growth factor and vascular endothelial growth factor, in the ovary. J Anim Sci 76:1671–1681.
Reynolds LP, Killilea SD, Redmer DA. 1992. Angiogenesis in the female reproductive system. FASEB J 6:886–892.
Reynolds LP, Grazul-Bilska AT, Redmer DA. 2002. Angiogenesis in the female reproductive organs: Pathological implications. Int J Exp Pathol 83:151–163.
Roland D, Ferder M, Kothuru R, Faierman T, Strauch B. 2000. Effects of pulsed magnetic energy on a microsurgically transferred vessel. Plast Reconstr Surg 105:1371–1374.
Ruggiero M, Bottaro DP, Liguri G, Gulisano M, Peruzzi B, Pacini S. 2004. 0.2 T magnetic field inhibits angiogenesis in chick embryo chorioallantoic membrane. Bioelectromagnetics 25: 390–396.
Saunders R. 2005. Static magnetic fields: Animal studies. Prog Biophys Mol Biol 87:225–239.
Schenck JF. 1996. The role of magnetic susceptibility in magnetic resonance imaging: MRI magnetic compatibility of the first and second kinds. Med Phys 23:815–850.
Shimizu E, Matsuda-Honjyo Y, Samoto H, Saito R, Nakajima Y, Nakayama Y, Kato N, Yamazaki M, Ogata Y. 2004. Static magnetic fields-induced bone sialoprotein (BSP) expression is mediated through FGF2 response element and pituitary-specific transcription factor-1 motif. J Cell Biochem 91: 1183–1196.
Shweiki D, Itin A, Soffer D, Keshet E. 1992. Vascular endothelial growth factor induced by hypoxia may mediate hypoxia-initiated angiogenesis. Nature 359:843–845.
Steinbrech DS, Mehrara BJ, Saadeh PB, Greenwald JA, Spector JA, Gittes GK, Longaker MT. 2000. VEGF expression in an osteoblast-like cell line is regulated by a hypoxia response mechanism. Am J Physiol Cell Physiol 278:C853–C860.
Szekanecz Z, Koch AE. 2001. Chemokines and angiogenesis. Curr Opin Rheumatol 13:202–208.
Szekanecz Z, Gaspar L, Koch AE. 2005. Angiogenesis in rheumatoid arthritis. Front Biosci 10:1739–1753.
Tepper OM, Callaghan MJ, Chang EI, Galiano RD, Bhatt KA, Baharestani S, Gan J, Simon B, Hopper RA, Levine JP, Gurtner GC. 2004. Electromagnetic fields increase in vitro and in vivo angiogenesis through endothelial release of FGF-2. FASEB J 18:1231–1233.
van Royen N, Piek JJ, Buschmann I, Hoefer I, Voskuil M, Schaper W. 2001. Stimulation of arteriogenesis; a new concept for the treatment of arterial occlusive disease. Cardiovasc Res 49: 543–553.
Veliks V, Ceihnere E, Svikis I, Aivars J. 2004. Static magnetic field influence on rat brain function detected by heart rate monitoring. Bioelectromagnetics 25:211–215.

Wagner PD. 2000. New ideas on limitations to VO_{2max}. Exerc Sport Sci Rev 28:10–14.

Williams CD, Markov MS, Hardman WE, Cameron IL. 2001. Therapeutic electromagnetic field effects on angiogenesis and tumor growth. Anticancer Res 21:3887–3891.

Winet H. 1996. The role of microvasculature in normal and perturbed bone healing as revealed by intravital microscopy. Bone 19:39S–57S.

Xu S, Okano H, Ohkubo C. 1998. Subchronic effects of static magnetic fields on cutaneous microcirculation in rabbits. In Vivo 12:383–389.

Xu S, Okano H, Ohkubo C. 2000. Acute effects of whole-body exposure to static magnetic fields and 50-Hz electromagnetic fields on muscle microcirculation in anesthetized mice. Bioelectrochemistry 53:127–135.

Xu S, Tomita N, Ohata R, Yan Q, Ikada Y. 2001. Static magnetic field effects on bone formation of rats with an ischemic bone model. Biomed Mater Eng 11:257–263.

Yamamoto Y, Ohsaki Y, Goto T, Nakasima A, Iijima T. 2003. Effects of static magnetic fields on bone formation in rat osteoblast cultures. J Dent Res 82:962–966.

Yan QC, Tomita N, Ikada Y. 1998. Effects of static magnetic field on bone formation of rat femurs. Med Eng Phys 20:397–402.

Yang HT, Ogilvie RW, Terjung RL. 1994. Peripheral adaptations in trained aged rats with femoral artery stenosis. Circ Res 74: 235–243.

Yuge L, Okubo A, Miyashita T, Kumagai T, Nikawa T, Takeda S, Kanno M, Urabe Y, Sugiyama M, Kataoka K. 2003. Physical stress by magnetic force accelerates differentiation of human osteoblasts. Biochem Biophys Res Commun 311:32–38.